ADA085138

(13)

AD

TECHNICAL REPORT
NATICK/TR-80/006

LEVEL II

A STUDY OF TRANSVERSELY LOADED PANELS USED IN TACTICAL SHELTERS

BY
ARTHUR R. JOHNSON

OCTOBER 1979

Approved for public release;
distribution unlimited.

UNITED STATES ARMY
NATICK RESEARCH and DEVELOPMENT COMMAND
NATICK, MASSACHUSETTS 01760

AERO-MECHANICAL
ENGINEERING LABORATORY

Approved for public release; distribution unlimited.

Citation of trade names in this report does not constitute an official indorsement or approval of the use of such items.

Destroy this report when no longer needed. Do not return it to the originator.

UNCLASSIFIED

SECURITY CLASSIFICATION OF THIS PAGE (When Data Entered)

REPORT DOCUMENTATION PAGE	READ INSTRUCTIONS BEFORE COMPLETING FORM
1. REPORT NUMBER: NATICK/TR-80/006 (14)	2. GOVT ACCESSION NO.: AD-A085 138
3. RECIPIENT'S CATALOG NUMBER	
4. TITLE (and Subtitle): A STUDY OF TRANSVERSELY LOADED PANELS USED IN TACTICAL SHELTERS (6)	5. TYPE OF REPORT & PERIOD COVERED
	6. PERFORMING ORG. REPORT NUMBER
7. AUTHOR(s): Arthur R. Johnson (10)	8. CONTRACT OR GRANT NUMBER(s): (12) 43
9. PERFORMING ORGANIZATION NAME AND ADDRESS: US Army Natick Research and Development Command, ATTN: DRDNA-UE, Natick, MA 01760	10. PROGRAM ELEMENT, PROJECT, TASK AREA & WORK UNIT NUMBERS: (17) 001, 62723A, 1L162723A427 01003BG (16)
11. CONTROLLING OFFICE NAME AND ADDRESS: US Army Natick Research and Development Command, ATTN: DRDNA-UE, Natick, MA 01760 (11)	12. REPORT DATE: Oct 79; 13. NUMBER OF PAGES: 43
14. MONITORING AGENCY NAME & ADDRESS (if different from Controlling Office): (1) Technical Reports	15. SECURITY CLASS. (of this report): UNCLASSIFIED; 15a. DECLASSIFICATION/DOWNGRADING SCHEDULE

16. DISTRIBUTION STATEMENT (of this Report)

Approved for public release; distribution unlimited

17. DISTRIBUTION STATEMENT (of the abstract entered in Block 20, if different from Report)

18. SUPPLEMENTARY NOTES

19. KEY WORDS (Continue on reverse side if necessary and identify by block number)

SANDWICH PANELS	HONEYCOMB STRUCTURES	FINITE ELEMENTS
ISO SHELTERS	STRUCTURAL BEHAVIOR	
ARMY SHELTERS	STRESSES	
HONEYCOMB SANDWICH PANELS	STRAIN MEASUREMENT	

20. ABSTRACT (Continue on reverse side if necessary and identify by block number)

A study of aluminum skin-honeycomb core sandwich panels was made. The objective was to determine the errors associated with using bending theory with linear transverse shear assumptions to describe the displacements, failure loads and skin strains for uniformly loaded rectangular sandwich panels. Available analysis techniques were used to predict data measured for large panels. Computed and measured vertical displacements were in good agreement. Computed failure loads based on core shear failure were found to be conservative for aluminum honeycomb cores. Computed and measured skin strains were also in good agreement. A finite

DD FORM 1 JAN 73 1473 EDITION OF 1 NOV 65 IS OBSOLETE

UNCLASSIFIED 392674

SECURITY CLASSIFICATION OF THIS PAGE (When Data Entered)

element analysis was made to determine the magnitude of error resulting from assuming the test panels were strictly simply supported.

PREFACE

This study represents a portion of the technical work being done at the US Army Natick Research and Development Command to validate analytical methods used for describing the structural behavior of tactical shelters. The finite element computations done to describe the behavior of complete shelter systems are based on standard theoretical assumptions of material behavior, that is, beam theory, plate theory, etc. Knowledge of the ability of the basic theories to predict reliable data is needed for meaningful processing of the finite element data on complete shelters. This study was done to determine the ability of plate bending theory (with linear transverse shear) to predict the bending response of large uniformly loaded rectangular panels placed over a rectangular void of nearly the same size as the panel.

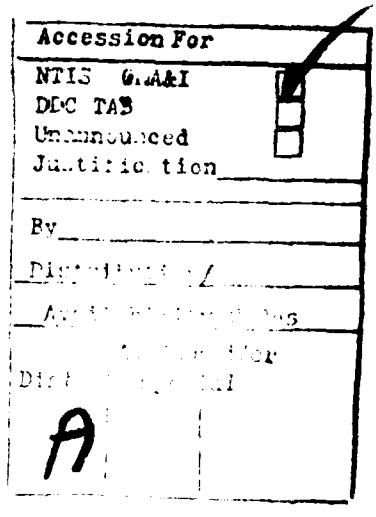

TABLE OF CONTENTS

LIST OF FIGURES

LIST OF TABLES

A STUDY OF TRANSVERSELY LOADED PANELS USED IN TACTICAL SHELTERS

1. INTRODUCTION:

During the development of prototype Army shelters it was determined that an accurate understanding of how sandwich panels behave in these shelters was necessary. With this accurate information designers are able to bring together technical knowledge of sandwich panel design methods and computed stress fields to evaluate a specific design. Design problems related to this study include the load-carrying capacity of wall, roof, and floor panels in Army shelters. Sandwich panels used in prototype shelters suffer from skin delamination. This shortens the life of the shelters. In order to improve and/or justify the design of these prototype shelters, reliable analytical methods are needed. The objective of this study is to investigate the accuracy of the sandwich panel theory (described in the appendix), when it is used to predict the bending response of panels commonly used in Army shelters.

Existing data on the response of sandwich panels made with thin aluminum skins and thick aluminun honeycomb cores is analyzed. The data includes measurements of the center deflections and skin strains and the failure loads for simply supported uniformly loaded rectangular panels. The data did not include measurements of the deflections and skin strains at locations other than the center of the panels. Tests to obtain distributional data for the aluminum skin and paper honeycomb core sandwich panels used in Army shelters were made. The existing test data and the new test data are analyzed in this report to demonstrate the ability of the sandwich panel theory described in the appendix to predict the measured data.

This study was done in conjunction with a finite element analysis of an Army shelter,[1] a test program measuring strains in large sandwich panels used in shelters,[2] and a test program measuring strains and accelerations in an environmentally loaded Army shelter.[3] This report contains data indicating that simple modeling techniques can be used to predict the bending response of the large sandwich panels used in Army shelters.

[1] A. R. Johnson and V. P. Ciras. Finite Element Analysis of a Statically Loaded ISO Tactical Shelter. Technical Report NATICK/TR–79/023, US Army Natick Research and Development Command, Natick, MA, 1979

[2] F. Barca. Experimental Measurement of Strain and Deflection in a Uniformly Loaded Simply Supported Composite Panel. Technical Report NATICK/TR–79/018, US Army Natick Research and Development Command, Natick, MA, 1978

[3] F. Barca. Experimental Measurement of Strain and Acceleration Levels in a Rigid-Wall Shelter Subjected to Environmental Loadings. Technical Report NATICK/TR–79/024, US Army Natick Research and Development Command, Natick, MA, 1978

2. COMPARISON OF THEORY AND EXPERIMENT:

a. Sandwich Panel Theory:

Sandwich panels have been extensively investigated and many theories have been proposed for the analysis of sandwich panels. The model used in this report is used in preference to more extensive models since the NASTRAN plate bending element is based on the same assumptions.[4] NASTRAN is being used for the analysis of complete shelters (see reference 1). Thus, knowledge of the agreement between measured and computed data based on this theory also applies to the finite element analysis made on complete shelters under other on-going efforts.

A summary of the crucial assumptions made in the theory is given as follows (the details of the theory are given in the appendix). The honeycomb core is assumed to act as a linear elastic solid. That is, the cellular structure of the core is ignored. An imaginary straight material line is assumed to exist through the panel. This line is assumed to rotate and remain straight as the panel deforms. The panels investigated in this report are not loaded in their planes and their out-of-plane deformations were less than 2.0% of the short span length. Thus, the theory assumes no in-plane stretching of the panels.

b. Aluminum Honeycomb Core Panels:

The development of a model for simply supported sandwich plates and a comparison of computed and measured data for simply supported rectangular sandwich plates was made in a series of reports issued by the Forest Products Laboratory.[5,6] The data in reference 6 for the panels loaded by a rubber bag is used in a new way in this section to study the accuracy of a simple bending and shear plate model for sandwich panels.

The panels tested in reference 6 consisted of square and rectangular panels. The square panels were 50.8 cm x 50.8 cm and the rectangular panels were 50.8 cm x 76.2 cm. The panels varied in thickness from 0.63 cm to 2.54 cm. The material used to make these panels was aluminum. The skins were made from 0.030–cm, 0.051–cm, or 0.081–cm–thick aluminum sheets and the aluminum honeycomb core was made from 0.0076–cm or 0.0127–cm aluminum–foil honeycomb.

[4] Richard H. MacNeal. The NASTRAN Theoretical Manual (Level 15), COSMIC, University of Georgia, Georgia, April 1972. Chapter 15.

[5] M. E. Raville. Deflection and Stresses in a Uniformly Loaded Simply Supported, Rectangular Sandwich Plate. Department of Agriculture, Forest Products Laboratory, No. 1847, December 1955

[6] W. C. Lewis. Supplement to Deflection and Stresses in a Uniformly Loaded, Simply Supported, Rectangular Sandwich Plate, Experimental Verification of Theory. Department of Agriculture, Forest Products Laboratory, No. 1847A, December 1956

Figures 1 and 2 contain plots of the relative error in the displacement of the center of the panels as a function of a flexibility constant R. The flexibility constant R is the ratio of the panel's shear flexibility to its total flexibility (computed from sandwich beam theory) in the short span direction of the panel.

$$R = \frac{F_S}{F_B + F_S}$$

where

$F_S = \frac{1}{8AG}$ = shear flexibility

$F_B = \frac{51^3}{384\,EI}$ = bending flexibility

1 = width of panel

A = cross-sectional area of core per m length of panel

E = modulus of skins

I = bending inertia of panel (from skins) per m length of panel

G = transverse shear modulus of core in width direction.

The relative error was computed assuming that the measured data was exact. These figures indicate that the errors were less than 10% with only one exception. This one data point is, of course, insufficient for determining if the theory is valid or not valid.

Figures 3 and 4 show that the relative errors found when predicting the failure load for the panels, based on core shear failure, are larger than the errors found in predicting the displacement at the center of the panel. Also, the errors appear to decrease as the value of R increases. The fact that the relative errors are negative is significant since this information alone indicates the panels failed at higher loads than anticipated from the theoretical calculations. Thus, the failure load calculations based on this simple theory were conservative for these panels. The possibility of the test apparatus introducing a clamping action at the boundary was mentioned in reference 6. In the next section of this report it is found that for the plates considered here the maximum shear strains are larger for clamped plates than for simply supported plates. Thus, since simply supported plates are stronger in shear than clamped plates, it is doubtful that the test apparatus edge constraints caused these errors. That is, if the test apparatus significantly increased the core shear strains at the boundary by introducing a clamping action, then the panels should have failed at lower loads than computed (but they actually failed at higher loads).

As mentioned above, the simple theory cannot explain the large errors associated with predicting the failure loads (core shear strain at edge of panel) by changing the boundary conditions used in obtaining the solution from simply supported to clamped. That is, the method of using ultimate core shear strength and core shear strains (at the center of the long

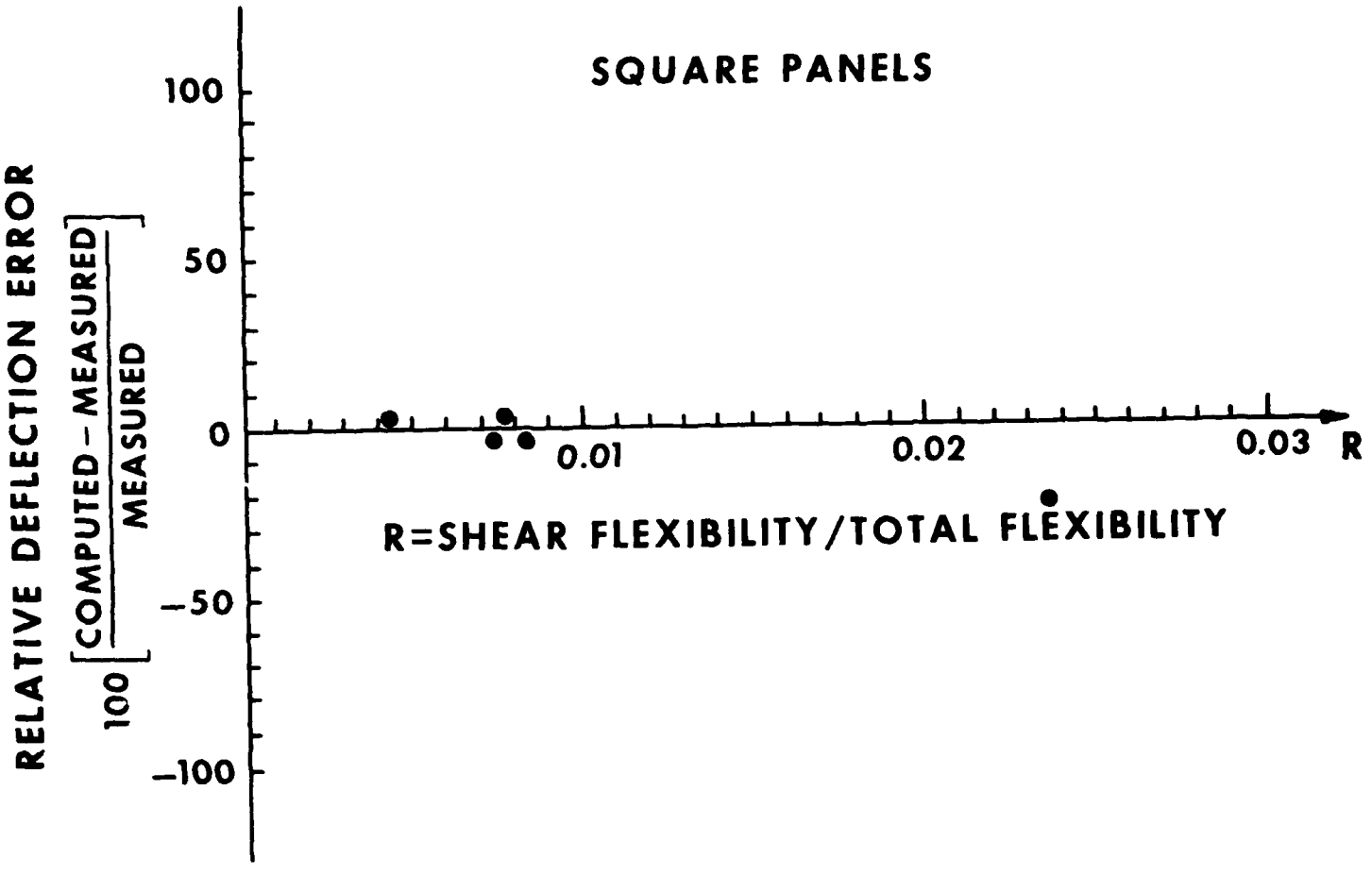

Figure 1 Deflection Error vs Flexibility Ratio, Square Panels

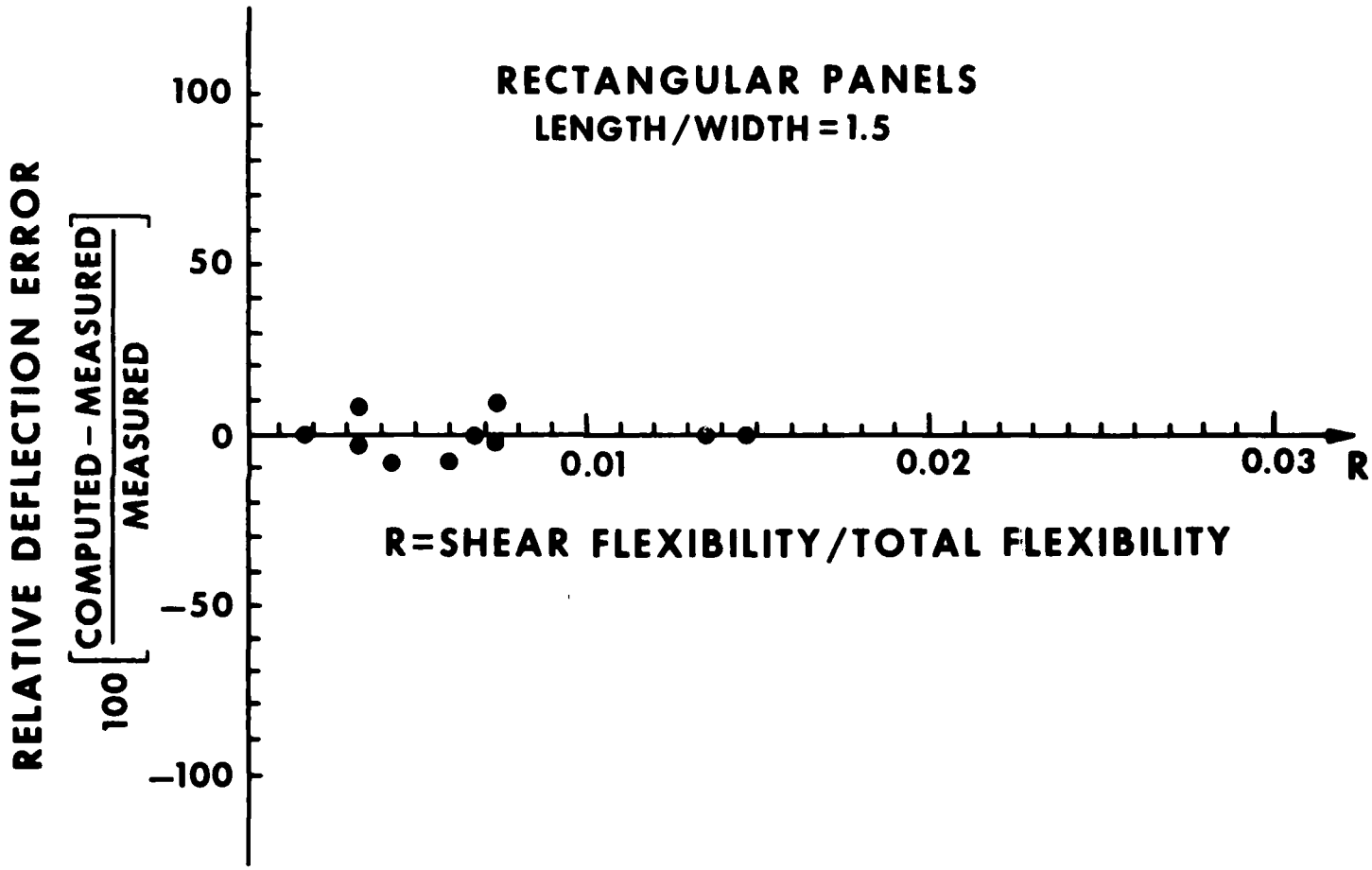

Figure 2 Deflection Error vs Flexibility Ratio, Rectangular Panels

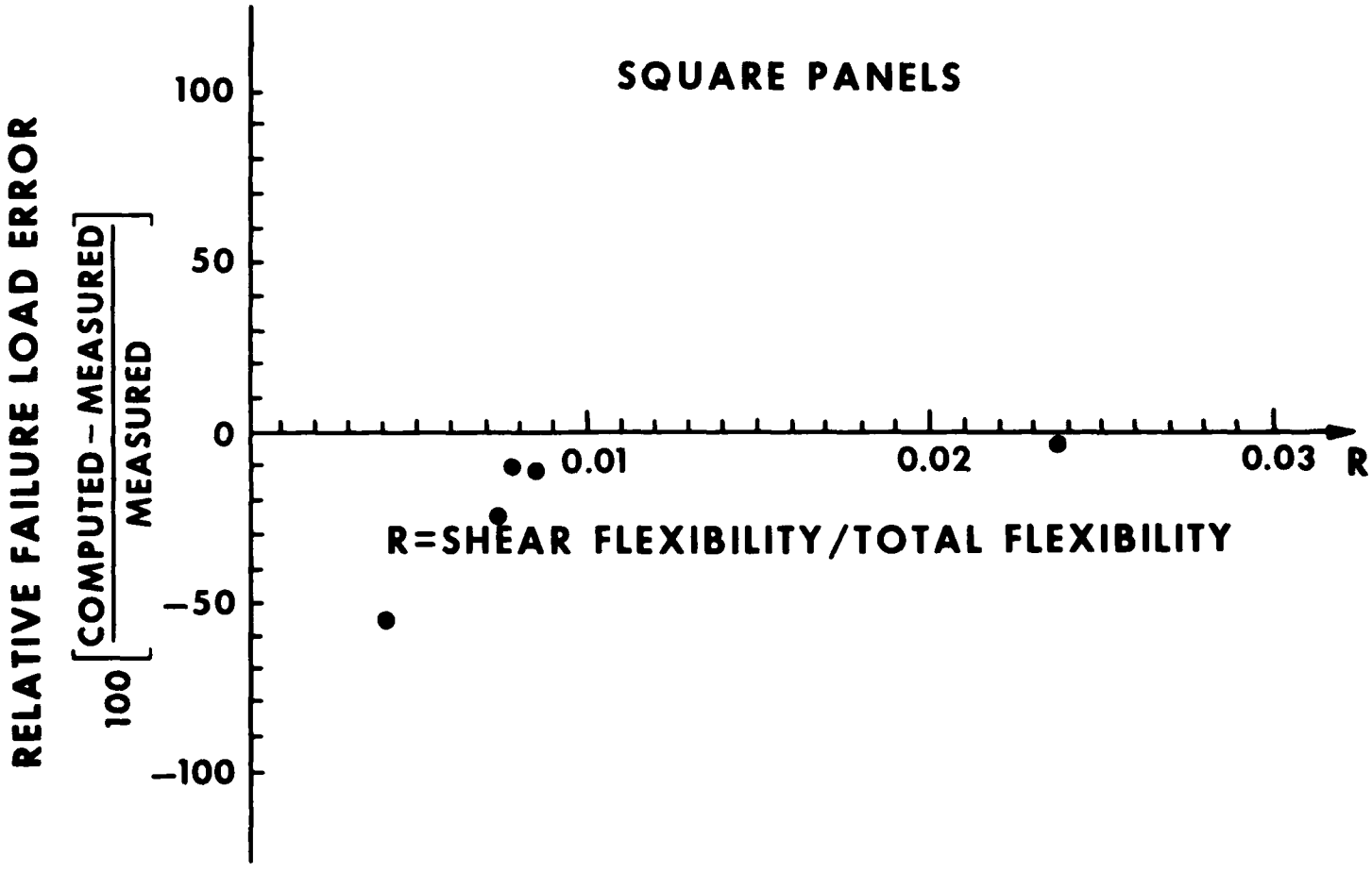

Figure 3 Failure Load Error vs Flexibility Ratio, Square Panels

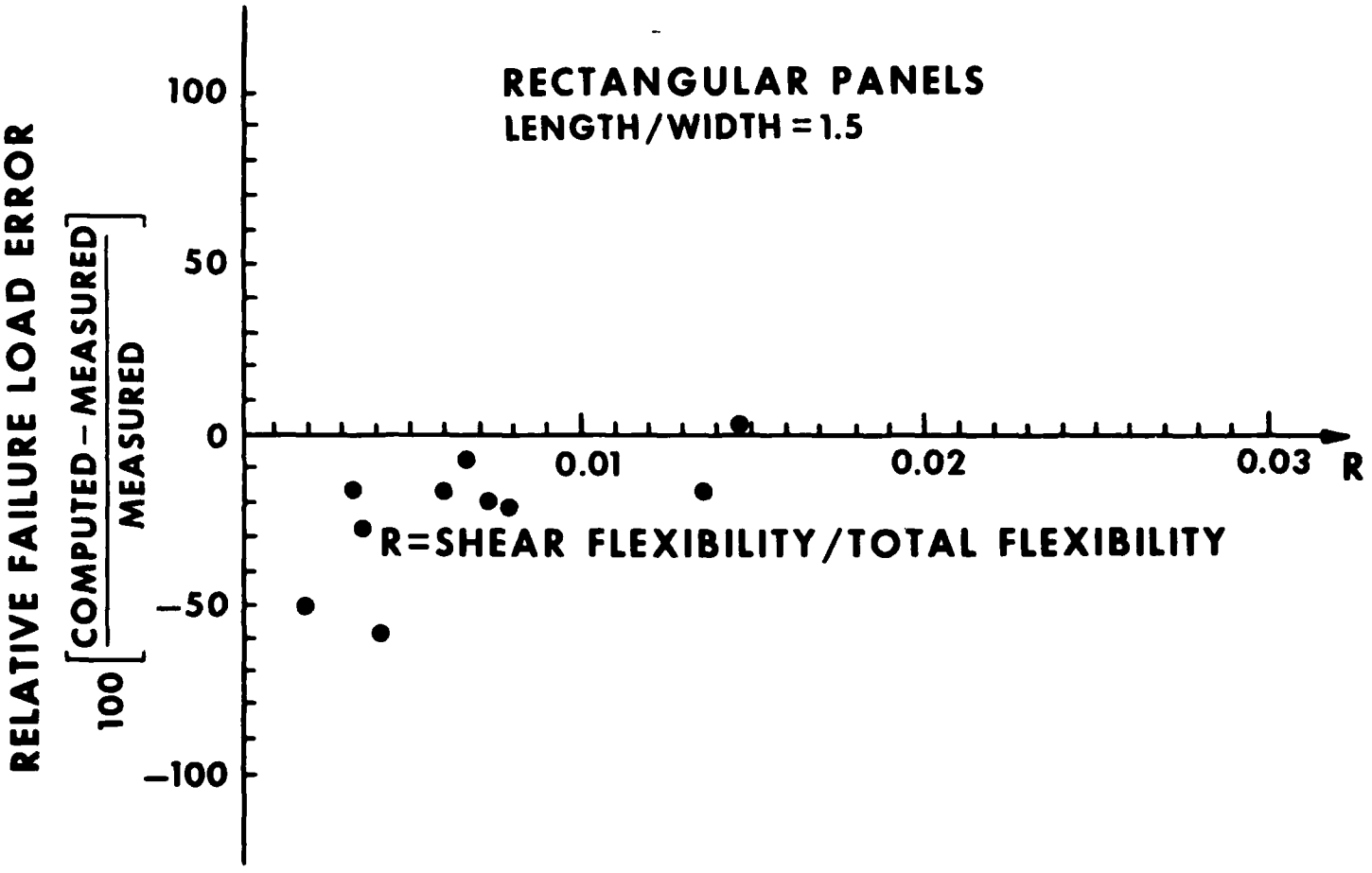

Figure 4 Failure Load Error vs Flexibility Ratio, Rectangular Panels

edge of the panels) predicted by the simple theory is not accurate. A more detailed study of what happens at the boundary and of the core properties is necessary if reliable panel failure loads are to be predicted.

It is interesting to note how the errors related to the panels' edge rotations Φ (Appendix) as computed by the simple theory. If these rotations are computed at the center of the long edge of each panel and if the errors are plotted against the center edge rotations, Figures 5 and 6 result. Figure 5 indicates that errors found when predicting the panels' center deflection (far from the boundary) had no relation to the edge rotations. However, Figure 6 indicates that the errors found when predicting the panels' failure loads using the maximum core shear strain at the boundary were related to the panel edge rotations. If the experimental equipment significantly restrained the panel edge rotations then the deflection errors would have been related to the edge rotations in Figure 5 as the failure load errors were related to the edge rotations in Figure 6. Computation by finite elements of the center deflection for panels restrained from rotation at the boundary, clamped, show that the center deflection is strongly related to the edge restraints for these panels.

c. Paper Honeycomb Core Panels:

The unexpected failure of paper honeycomb sandwich panels in early prototype shelters resulted in a loss in confidence in design calculations for these panels. Often detailed analysis of these prototype shelters was not possible or was not documented. Thus, there was little technical information available on the behavior of the actual panels being used in the shelters. Some of the technical information that did exist[7] indicated large variations in the mechanical properties of the paper honeycomb core materials. In this section a study is made of six different types of aluminum skin-paper honeycomb core sandwich panels. Large panels with the actual materials used in the prototype shelters were fabricated and tested (see reference 2). The experimental data is compared to the sandwich panel theory described in the appendix. The purpose of this comparison is to determine the degree to which the simple analysis techniques can describe the behavior in an actual bending problem.

To assure that errors were not introduced by improperly modeling the panel geometry or core properties, a series of measurements were made to check the panel geometry and core properties. The results of the core property measurements are given in reference 2. Two panels (panels No. 2 and No. 10 in reference 2) were checked for correct total thickness and correct skin thickness. The assumed total thickness of the first panel was 5.283-cm and the average (and standard deviation) thickness was found to be 5.286 ± 0.005-cm. The assumed total thickness of the second panel was 9.119-cm and the average thickness was found to be 9.134 ± 0.005-cm. Samples of the aluminum skins were also checked. The skins assumed to be 0.1016-cm thick were found to have an average thickness of 0.102 ± 0.002-cm. The skins assumed to be 0.1270-cm thick were found to be 0.130 ± 0.002-cm thick. A study

[7] T. W. Reichard. Mechanical Properties of Paper Honeycomb for Use in Military Shelters. NBS Report 10544, National Bureau of Standards Washington, DC, February 1971

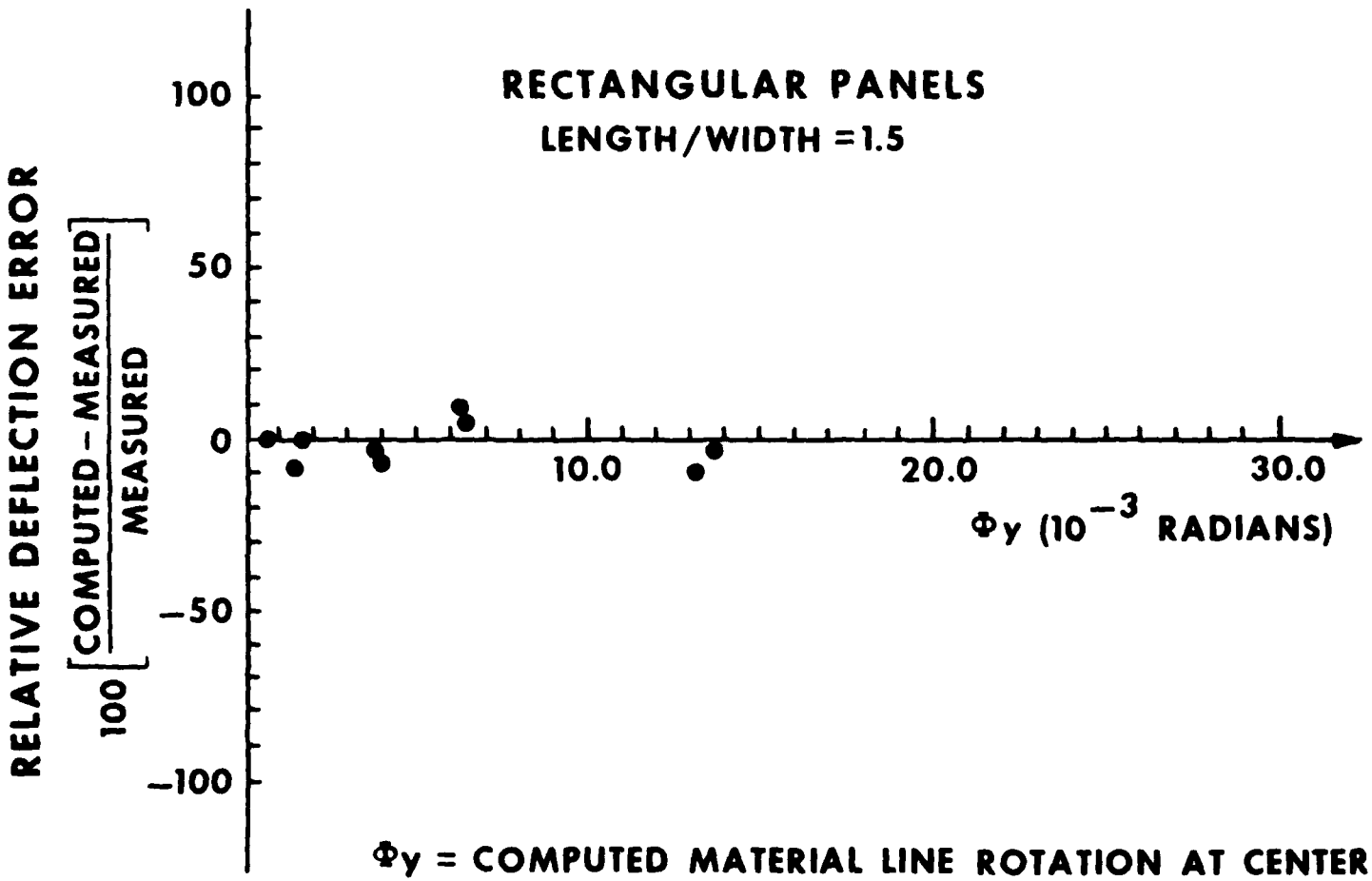

Φy = COMPUTED MATERIAL LINE ROTATION AT CENTER OF LONG EDGE OF PANELS IN RADIANS.

15

Deflection Error vs Material Line Rotation, Rectangular Panels

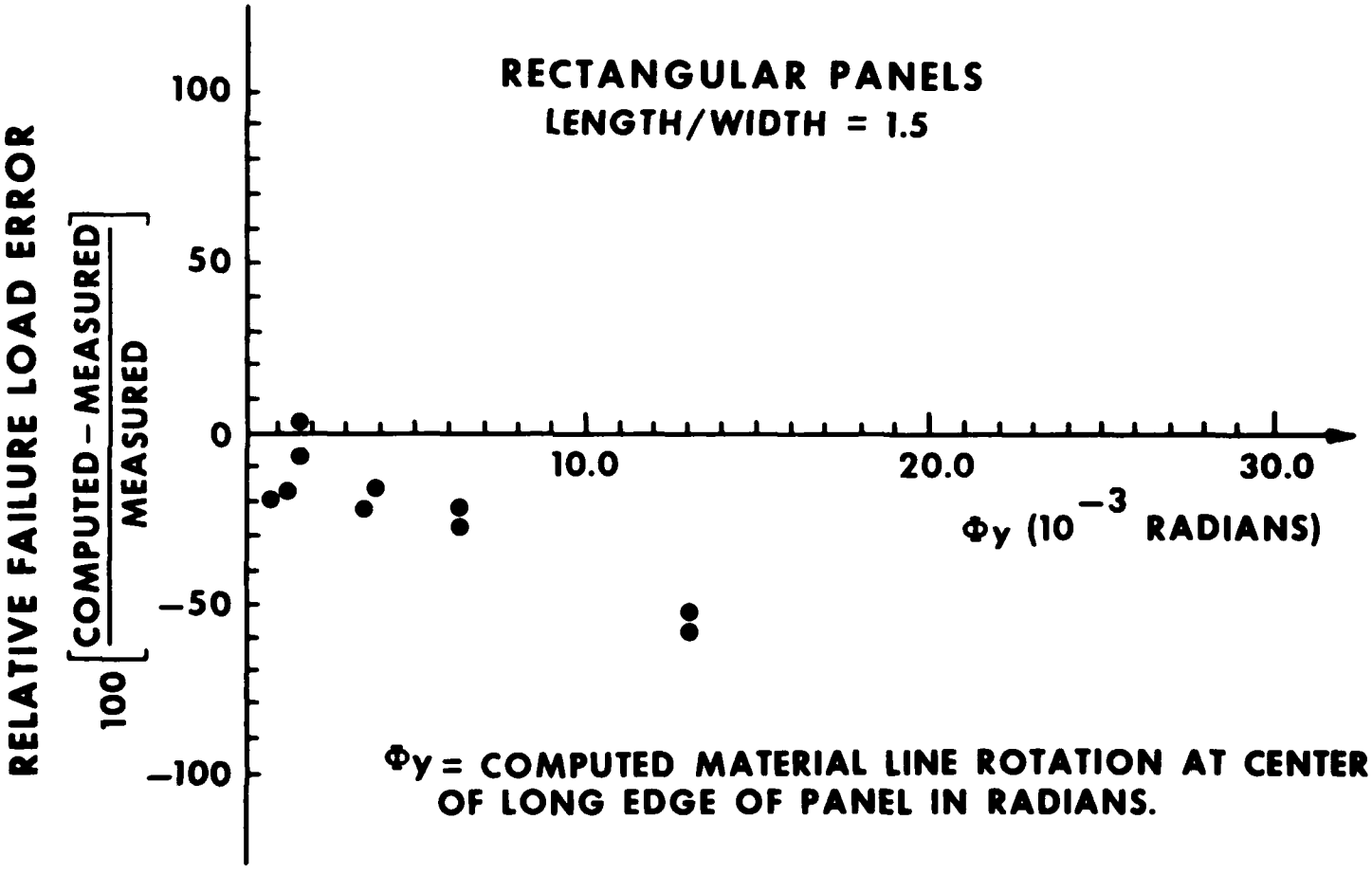

Figure 6 Failure Load Error vs Material Line Rotation, Rectangular Panels

of computed and measured strain and displacement data indicates the computed errors were much too large to be related to the dimensional errors cited above in the total panel thickness and skin thickness.

Since the panels' top skins were in compression and the bottom skins were in tension, the compressional and tensile elastic properties of the 5052-H34/H36 aluminum skins were obtained from MIL-HDBK-5C.[8] The modulus of this material in compression is 7.032×10^{10} Pa and in tension it is 6.964×10^{10} Pa. The shear modulus, G, in each case was computed using $G = E/2(1 + \nu)$ where $\nu = 0.33$ Poisson's ratio for aluminum and E is the compression or tension modulus.

As a result of studying the mechanical properties of paper honeycomb, Reichard (see reference 7) discovered that the core shear modulus changes significantly with core thickness. Since 1.27-cm thick samples were used to determine the core properties (see reference 2) and since the cores are 5.283-cm and 9.115-cm thick, correction factors must be applied to the core shear modulus values measured. Figure 13 or reference 7 was used to estimate correction factors with linear extrapolation. Correction factors of 0.75 and 0.67 were obtained for the 5.283-cm and 9.119-cm thick panels analyzed in this study. These represent 75% and 67% reduction in stiffness over that of the 1.27-cm thick samples. Thus, after adjusting for thickness, the core properties for the 5.283-cm thick panels are 1.112×10^8 Pa and 5.309×10^7 Pa for the TL and TW directions, respectively. The core properties for the 9.119-cm thick panels are 9.936×10^7 Pa and 4.742×10^7 Pa for the TL and TW directions, respectively.

The test data reported in reference 2 was measured at fourteen locations on the panel. The X and Y coordinates of the data recovery points are indicated in Figure 7. Strain measurements were made on both the top and bottom of the panel at the seven X and Y locations shown. There were six types of panels tested and there were two panels of all but one type. Three panels were 5.283-cm thick and eight were 9.119-cm thick. All the panels had 60.9 kg/m^3, MIL-H-21040, 11.1-mm cell Kraft paper honeycomb cores, and various combinations of 1.016-mm and 1.0270-mm thick 5052-H34/H36 aluminum skins. The panels were classified by their shear flexibility to total flexibility ratio (measured in the short span direction), R, for comparing computed and measured data in this section. The relation between the R vales and the panel numbers of reference 2 is given in Table 1.

The results of comparing the measured and computed vertical deflections is given in Table 2. In constructing Table 2, data for a 60-kPa loading from reference 2 was used. This table and Tables 3 through 6 are set up similarly to Figure 7 so that the errors near the center of a panel can be easily compared with the errors near the edges. The errors at locations 6 and 7 in Figure 7 are discussed in section 3b. The data in Table 2 indicate that there was good agreement between the computed displacements and measured displacements at locations 1 through 5. A negative relative error indicates that the measured value was larger than the computed value. Most of the errors were negative.

[8]Military Standardization Handbook MIL-HDBK-5C, Metallic Materials and Elements for Aerospace Vehicle Structures, 15 September 1976.

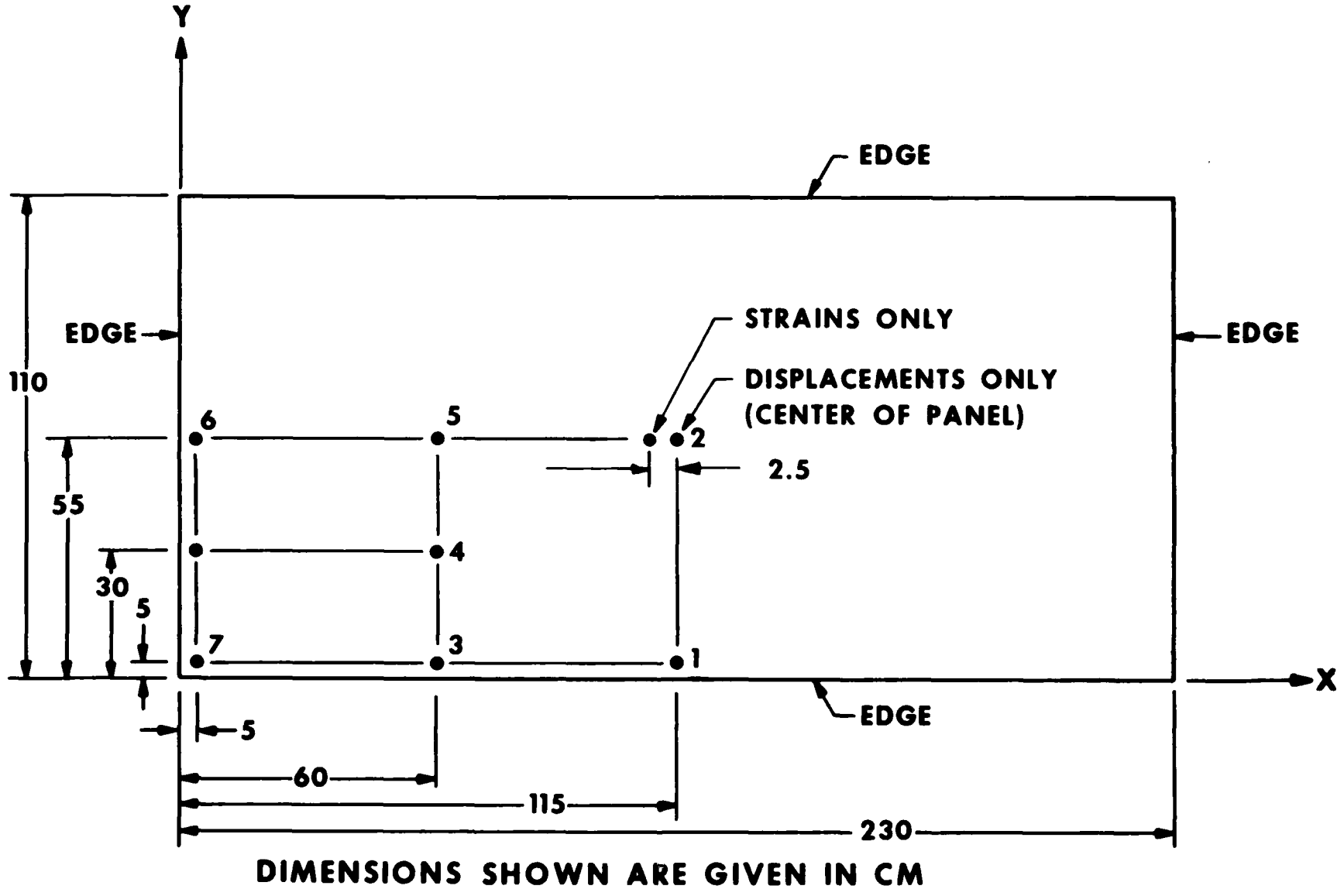

Figure 7 Strain and Displacement Locations

TABLE 1

R Values of Panels vs Panel Numbers Given in Reference 2

Panel Numbers	R
1, 2	0.0284
3, 4	0.0138
5, 6	0.0662
7, 8	0.0327
9, 10	0.0591
11, 12	0.0291

TABLE 2

Displacement Errors*

Pressure = 60 kPa
R = Shear Flexibility/Total Flexibility
(i) = Location No. i. See Figure 12.

$$\% \text{ Error} = 100\left[\frac{\text{Computed} - \text{Measured}}{\text{Measured}}\right]$$

	R		X = 0.05 m (Edge)		X = 0.60 m (Quarter)		X = 1.15 m (Center)
Y = 0.55 m (Center)	0.0138	(6)	-48.2, -64.2	(5)	-10.5, -11.7	(2)	-7.5, - 9.9
	0.0284		-62.8 —		- 5.8 —		0.3 —
	0.0291		-68.9, -65.4		-15.8, -16.5		- 8.9, -13.9
	0.0327		-61.0, -63.2		-11.8, - 9.1		- 4.3, - 3.5
	0.0591		-67.7, —		- 8.1, - 4.7		0.5, 0.2
	0.0662		-73.6, -71.9		- 6.0, - 2.8		3.5, - 0.5
Y = 0.30 m (Quarter)	0.0138			(4)	-11.3, -12.6		
	0.0284				- 6.5 —		
	0.0291				-16.2, -16.9		
	0.0327				-11.9, - 9.1		
	0.0591				- 6.7, - 4.0		
	0.0662				- 6.1, - 4.4		
Y = 0.05 m (Edge)	0.0138	(7)	-56.2, -64.4	(3)	-12.0, -16.4	(1)	-11.0, -11.2
	0.0284		-64.8 —		- 4.8 —		- 7.1 —
	0.0291		-64.7, -62.4		-12.9, -22.7		-10.2, -16.4
	0.0327		-58.3, -60.5		-12.2, -10.0		- 4.6, - 5.5
	0.0591		-37.8, -43.2		- 8.4, - 2.5		- 1.8, 13.7
	0.0662		-65.7, -60.7		- 0.5, - 9.2		2.2, - 1.8

*NOTE: See Section 3 for comments on errors at locations 6 and 7.

Tables 3 and 4 list the relative errors for the skin strains in the short span direction for both the bottom and top skins. It is interesting to note that the panels which were fabricated with equal skins did not have the strains on the bottom skin equal to the strains on the top skin. When the compression modulus and tensile modulus of the aluminum skins were used for the top and bottom skins, the theory also predicted that the top and bottom skins would not have equal strains. However, out of the seven symmetrical panels tested, only two agreed with the theoretical prediction (at the center of the panel) that the top skin would have a lower strain than the bottom skin. Tables 3 and 4 indicate that the computed and measured skin strains in the short span direction do not agree as well as the computed and measured displacements for locations 1, 3, 4, and 5. The relative strain errors at location 2 indicate good agreement at the center of the panel with the strains being under-predicted by the theory. The errors indicated at location 1 appear to be random. Tables 5 and 6 list the relative errors for the skin strains in the long span direction. These tables indicate poor agreement between measured strains and theoretically computed strains at locations 1 through 5.

3. FINITE ELEMENT SOLUTIONS WITH NASTRAN (LEVEL 15.5):

a. Simply Supported and Clamped Rectangular Sandwich Panels:

The analysis of a complete shelter subjected to arbitrary loading and boundary conditions requires the use of finite element theory. As mentioned in section 2, the NASTRAN CQDPLT element accuracy was of concern in this effort. Thus, the following work represents the computations made to check the accuracy of solutions obtained with the CQDPLT element relative to the results of the sandwich plate theory. As shown in the appendix, the CQDPLT element is based on the same theoretical assumptions as the sandwich plate theory except that the CQDPLT element allows for only isotropic transverse shear properties.

Uniformly loaded, simply supported, rectangular sandwich panels were considered. The panels' center deflections and their material line rotations at the center of their long edges were the variables chosen for this comparison study. Figure 8 shows the relation between the finite element mesh sizes, the panel dimensions, and the variables w and Φ_y (the center deflection and the rotation at the center of the long edge, respectively). For the plate bending problem data on the convergence of finite element solutions to an analytical solution is presented in the NASTRAN literature (see reference 4). Since the NASTRAN element allows for only isotropic transverse shear properties, and since actual panels have orthotropic transverse shear properties there is a question of what core material properties should be used in the finite element analysis. Analytical and finite element solutions were computed considering panels with different R values and considering different core properties in the finite element solutions. The data generated is used below to describe the magnitude of the errors realized when finite element solutions are compared to the analytical solutions.

Three rectangular panels with flexibility ratios, R, of 0.0011, 0.0065, and 0.0135 and a length to width ratio of 1:5 were analyzed. The analytical solutions were made considering the two different core transverse shear properties (see appendix). The finite element solutions were made by computing the plate bending inertia to three significant figures and using the core shear modulus in the short span direction. The mesh was refined in a uniform manner

TABLE 3

Strain Errors Short Span Direction, Bottom Skins*

Pressure = 60 kPa
R = Shear Flexibility/Total Flexibility
(i) = Location No. i. See Figure 12.

	R	% Error = 100 [Computed − Measured / Measured]		
		X = 0.05 m (Edge)	X = 0.60 m (Quarter)	X = 1.125 m (Center)
Y = 0.55 m (Center)	0.0138	(6) −, -74.4	(5) 6.2, -13.6	(2) - 6.4, - 7.7
	0.0284	-76.1, −	-11.7, −	- 5.3, −
	0.0291	-79.5, -81.8	-17.8, -18.4	-13.1, -12.5
	0.0327	-81.0, -81.7	-16.0, -11.6	- 8.5, - 3.3
	0.0591	-86.6, -86.2	-18.4, -14.8	- 8.6, - 7.0
	0.0662	-85.3, -87.5	-12.3, -16.3	4.2, 0.0
Y = 0.30 m (Quarter)	0.0138		(4) -12.9, -15.1	
	0.0284		- 8.5, −	
	0.0291		-17.5, -18.7	
	0.0327		-17.7, -13.2	
	0.0591		-15.6, -16.8	
	0.0662		-11.6, - 9.1	
Y = 0.05 m (Edge)	0.0138	(7) -74.9, -70.2	(3) -11.5, -25.8	(1) - 6.2, -17.1
	0.0284	-83.1, −	5.4, −	22.8, −
	0.0291	-70.5, -68.9	-13.5, -19.0	-20.6, -18.0
	0.0327	-66.2, -64.6	-32.1, 4.0	7.9, 10.2
	0.0591	-75.5, -85.9	24.4, -23.3	65.5, -35.0
	0.0662	-56.7, -77.6	-26.5, 54.2	-246.8, 46.8

*Note: See Section 3 for comments on errors at locations 6 and 7.

TABLE 4

Strain Errors Short Span Direction, Top Skins*

Pressure = 60 kPa
R = Shear Flexibility/Total Flexibility
(i) = Location No. i. See Figure 12.

$$\% \text{ Error} = 100 \left[\frac{\text{Computed} - \text{Measured}}{\text{Measured}} \right]$$

	R	X = 0.05 m (Edge)	X = 0.60 m (Quarter)	X = 1.125 m (Center)
Y = 0.55 m (Center)	0.0138	(6) -75.6, -77.0	(5) -14.7, -16.2	(2) -12.7, -14.4
	0.0284	-79.5, –	-18.5, –	-12.6, –
	0.0291	-81.8, -82.1	-17.1, -19.0	-11.6, -12.7
	0.0327	-81.7, -81.0	-15.1, -12.6	- 9.0, - 4.9
	0.0591	-85.6, -86.4	-21.7, -19.9	-12.1, - 7.8
	0.0662	-86.4, -87.8	-14.8, -23.2	24.2, -11.2
Y = 0.30 m (Quarter)	0.0138		(4) -16.0, -16.7	
	0.0284		-16.9, –	
	0.0291		-18.0, -17.9	
	0.0327		-19.4, -13.8	
	0.0591		-20.2, -24.4	
	0.0662		– -20.8	
Y = 0.05 m (Edge)	0.0138	(7) -69.5, -63.0	(3) -10.4, -24.6	(1) - 4.0, - 4.3
	0.0284	-83.8, –	-20.0, –	25.7, –
	0.0291	-65.5, -66.3	-28.1, -23.6	0.5, -16.1
	0.0327	-64.6, -51.1	-34.9, 2.4	5.7, 24.2
	0.0591	-77.9, -85.1	1.5, -38.2	62.3, -35.6
	0.0662	-152. , -79.7	59.4, 34.1	2.3, 38.8

*Note: See Section 3 for comments on errors at locations 6 and 7.

TABLE 5

Strain Errors Long Span Direction, Bottom Skins*

Pressure = 60 kPa
R = Shear Flexibility/Total Flexibility
(i) = Location No. i, See Figure 12

$$\% \text{ Error} = 100 \frac{\text{Computed} - \text{Measured}}{\text{Measured}}$$

	R	(6)	(5)	(2)
Y = 0.55 m (Center)	0.0138	–, -24.1	- 25.7, -17.6	-39.1, -51.3
	0.0284	19.2, –	- 2.9, –	-13.7, –
	0.0291	183.3, 45.7	- 15.3, - 1.6	-32.3, -13.7
	0.0327	- 5.7, 25.0	- 50.6, -49.6	-67.7, -68.4
	0.0591	273.7, 787.5	- 2.5, -15.1	-15.8, -36.2
	0.0662	-182.6, -1114.3	185.5, - 2.1	19.7, -25.1
			(4)	
Y = 0.30 m (Quarter)	0.0138		- 24.9, -12.1	
	0.0284		- 1.5, –	
	0.0291		- 9.4, 15.7	
	0.0327		- 56.0, -53.3	
	0.0591		- 16.9, -25.6	
	0.0662		1.7, - 8.1	
		(7)	(3)	(1)
Y = 0.05 m (Edge)	0.0138	- 83.6, -87.0	- 59.1, -65.4	-78.4, -70.5
	0.0284	- 63.8, –	30.0, –	43.8, –
	0.0291	- 86.4, -85.7	- 71.0, -69.5	-89.3, -87.1
	0.0327	- 91.1, -88.9	- 87.8, -89.9	-95.8, -95.3
	0.0591	- 74.6, -63.3	- 70.4, -83.6	-88.8, -89.0
	0.0662	- 68.9, - 78.9	- 59.3, -70.3	38.9, -84.9
		X = 0.05 m (Edge)	X = 0.60 m (Quarter)	X = 1.125 m (Center)

*NOTE: See Section 3 for comments on errors at locations 6 and 7.

TABLE 6

Strain Errors Long Span Direction, Top Skins*

Pressure = 60 kPa
R = Shear Flexibility/Total Flexibility
(i) = Location No. i, See Figure 12

$$\% \text{ Error} = 100 \left[\frac{\text{Computed} - \text{Measured}}{\text{Measured}} \right]$$

	R	(7)	(5)	(2)
Y = 0.55 m (Center)	0.0138	-9.9, -8.5	-11.3, 0.9	-18.2, 44.0
	0.0284	42.0, —	15.9, —	15.8, —
	0.0291	950.0, 6200.	- 3.1, 15.4	-14.1, 3.8
	0.0327	8.9, - 476.9	-47.8, 47.1	-66.4, -66.9
	0.0591	-341.7, 141.7	2.1, -12.5	-18.5, 29.3
	0.0662	268.4, 511.8	23.2, - 2.5	241.2, -20.2
Y = 0.30 m (Quarter)	0.0138		-14.4, -11.9	
	0.0284		5.0, —	
	0.0291		5.3, 20.2	
	0.0327		-55.0, -50.3	
	0.0591		-16.7, -22.3	
	0.0662		123.8, -17.1	
Y = 0.05 m (Edge)	0.0138	-85.3, -88.8	-79.1, -80.3	-89.4, -86.0
	0.0284	-67.0, —	-55.6, —	-66.4, —
	0.0291	-84.9, -83.6	-73.8, -78.6	-92.6, -90.6
	0.0327	-90.0, -89.6	-88.6, -92.1	-96.2, -95.9
	0.0591	-69.3, -64.6	-78.7, -85.9	-91.5, -85.9
	0.0662	-53.8, -75.3	- 7.9, -73.5	-84.1, -88.4
		X = 0.05 m (Edge)	X = 0.60 m (Quarter)	X = 1.125 m (Center)

*NOTE: See Section 3 for comments on errors at locations 6 and 7.

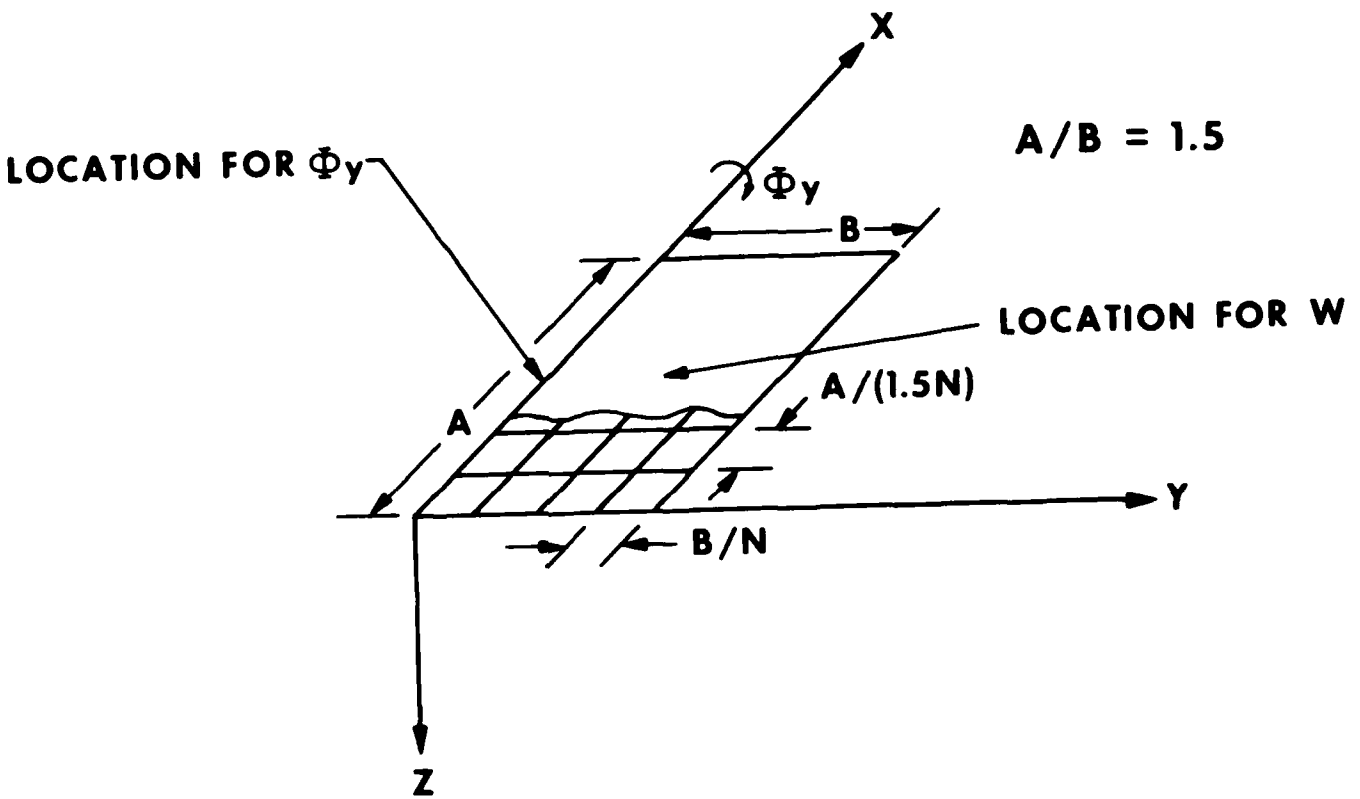

Figure 8 Finite Element Mesh for Comparison Calculations

as indicated in Figure 8. The results of the computations are shown in Figures 9, 10, and 11. These figures indicate that the finite element solutions are nearly converged if the short side contains four or more elements. Also, we have the following quantitative description of some qualitatively expected results. If the largest core shear modulus is used (Figure 9 and 10) the finite element solutions give smaller displacements than the analytical solutions by as much as 10%. If the smallest core shear modulus is used (Figure 11) the finite element solutions give larger displacements than the analytical solutions by as much as 10%. These figures indicate one type of numerical information which a shelter designer using the finite element technique should have when he is studying the finite element model.

Computations were made by the finite element method using a 12 x 18 mesh for uniformly loaded clamped rectangular panels with flexibility ratios, R, of 0.0011 and 0.0135 and a length to width ratio of 1.5. These computations were made to investigate the shear strain distribution along the long edge of the panel for both simply supported and clamped panels. The simply supported shear strain distribution data was taken from an analytical solution which used the same isotropic core properties used in the finite element analysis. The results are given in Figure 12. It was found that the maximum core shear strain on the long edge of the panel increases when the boundary conditions are changed from simply supported to clamped. In fact, the increase was about 50% for the panel with a flexibility ratio, R, of 0.0011. This information (clamped panel's core shear strains along the long edge) is useful to designers making general design recommendations based on handbook formulas valid only for simply supported sandwich panels. The data in Figures 9 to 10 indicates that insofar as predicting the displacements (w and Φ_y) are concerned, the actual transverse shear modulus used in the finite element model can affect the computed displacements by more than 10.0%.

b. Rectangular Sandwich Panel Resting on a Rectangular Void:

The finite element solutions for the simply supported uniformly loaded panels contained corner "hold-down forces." The panel corners were not held down in the experiment. As a result, the corners of the panel would curl up in the experiment and the measured data near the end of the panel would not apply to the case of a simply supported panel. To study the magnitude of the errors resulting from the panel curling up in the corners the finite element method was used to compute displacement and strain data 5.0-cm from the end of panels 1 and 2 (see reference 2 for panel data). The case when the panels are simply supported and the case when the panels are allowed to curl off of the foundation in the corner were analyzed.

In the finite element analyses a uniform mesh (see Figure 8) with 12 divisions in the short span direction and 18 divisions in the long span direction was used. The first analysis was made using simply supported boundary conditions. The second analysis was made with the same boundary conditions as the first except the four corner nodes were allowed to move vertically. The remainder of the analyses was made by allowing the nodes which had hold-down forces in a previous analysis to be free in the vertical direction. Only one solution was found with no hold-down forces. This solution had the corner nodes and one node each side of the corner free to move in the vertical direction.

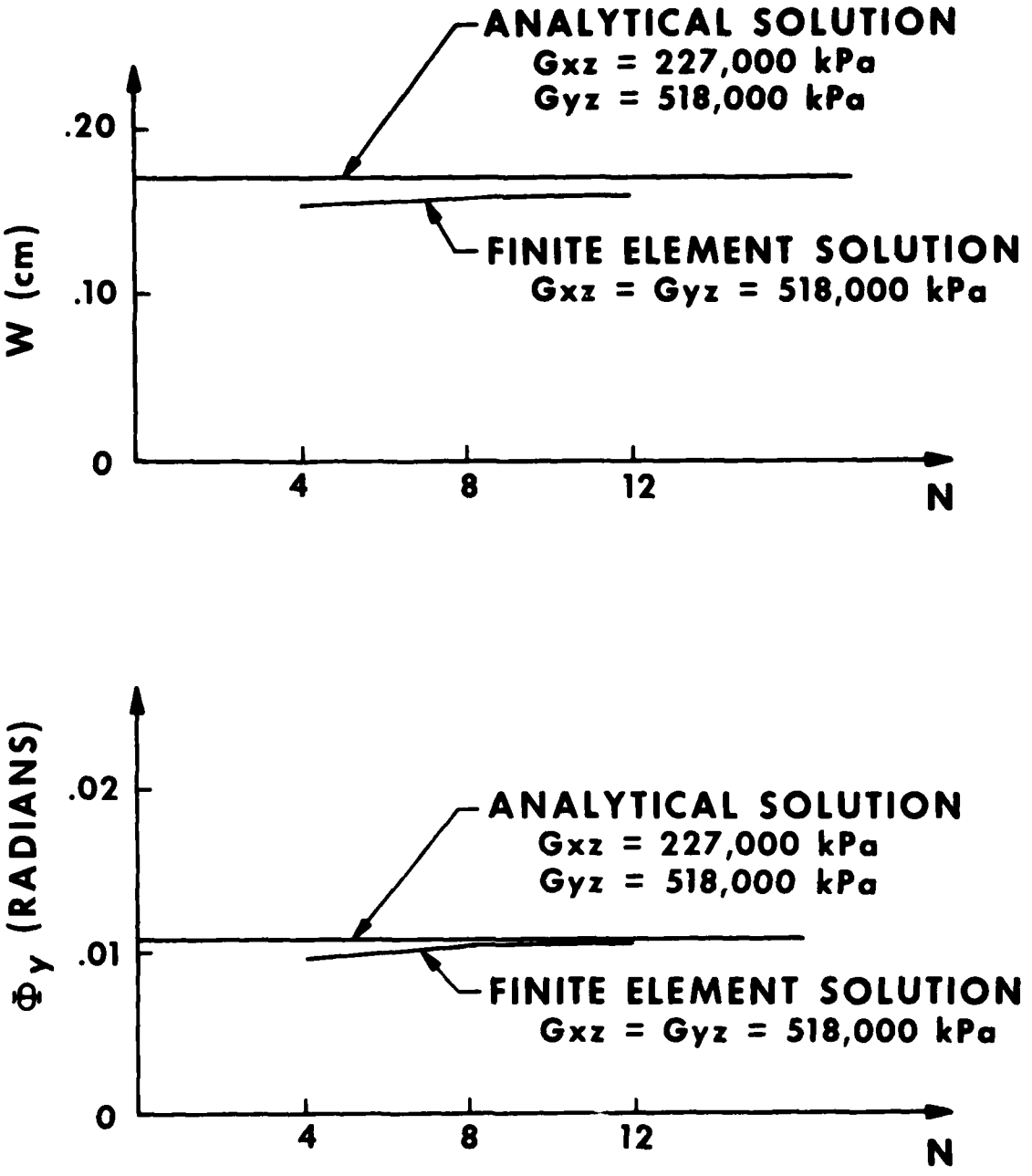

N = NUMBER OF ELEMENTS ON SHORT SIDE OF PLATE
W = VERTICAL DEFLECTION AT CENTER OF PLATE
Φ_y = ROTATION OF MATERIAL LINE AT CENTER OF LONG EDGE OF PLATE

Figure 9 Comparison of Analytical and Finite Element Solutions. R = 0.0011

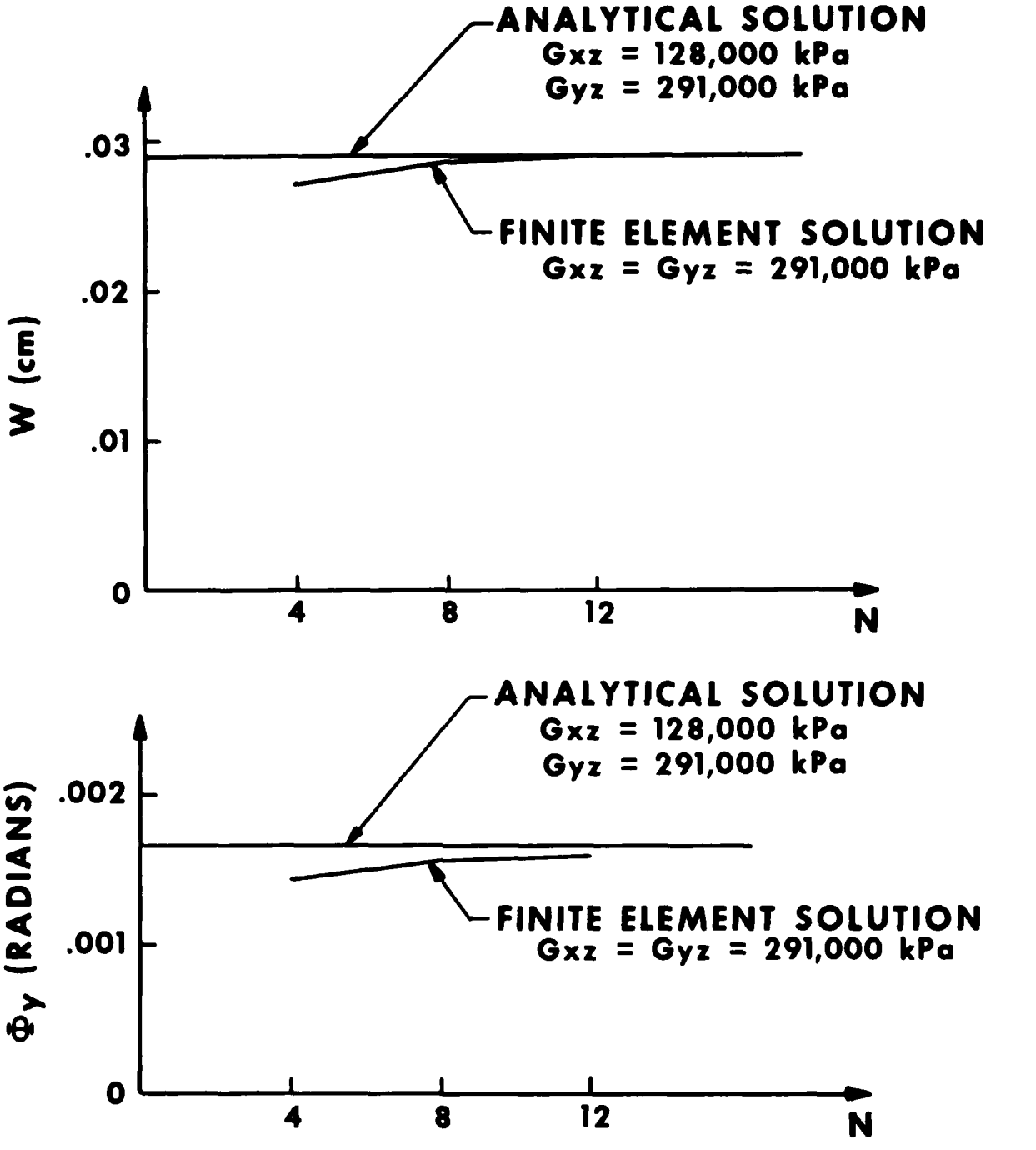

N = NUMBER OF ELEMENTS ON SHORT SIDE OF PLATE

W = VERTICAL DEFLECTION AT CENTER OF PLATE

Φ_y = ROTATION OF MATERIAL LINE AT CENTER OF LONG EDGE OF PLATE

Figure 10 Comparison of Analytical and Finite Element Solutions. R = 0.0065

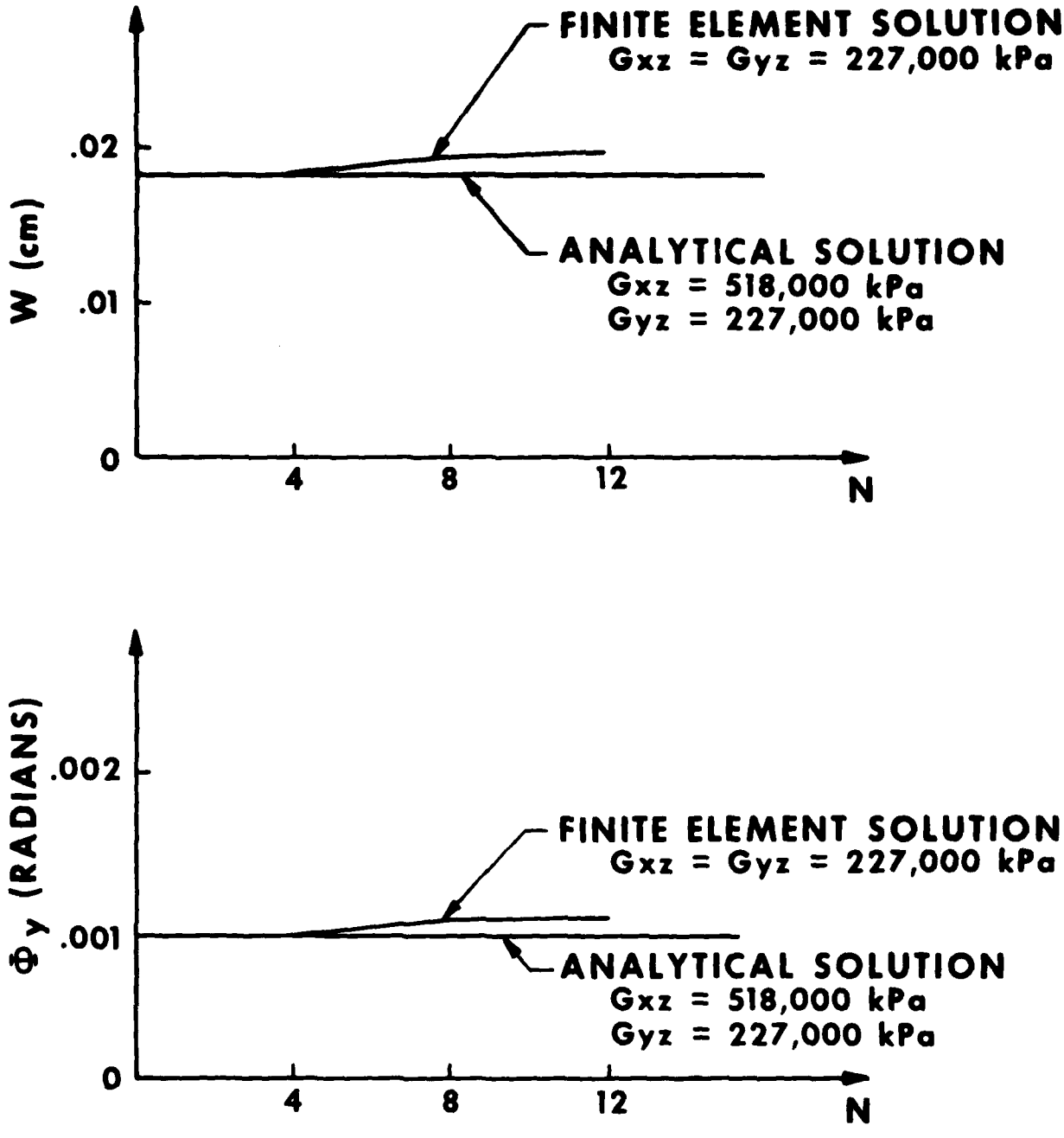

N = NUMBER OF ELEMENTS ON SHORT SIDE OF PLATE

W = VERTICAL DEFLECTION AT CENTER OF PLATE

Φy = ROTATION OF MATERIAL LINE AT CENTER OF LONG EDGE OF PLATE

Figure 11 Comparison of Analytical and Finite Element Solutions. R = 0.0135

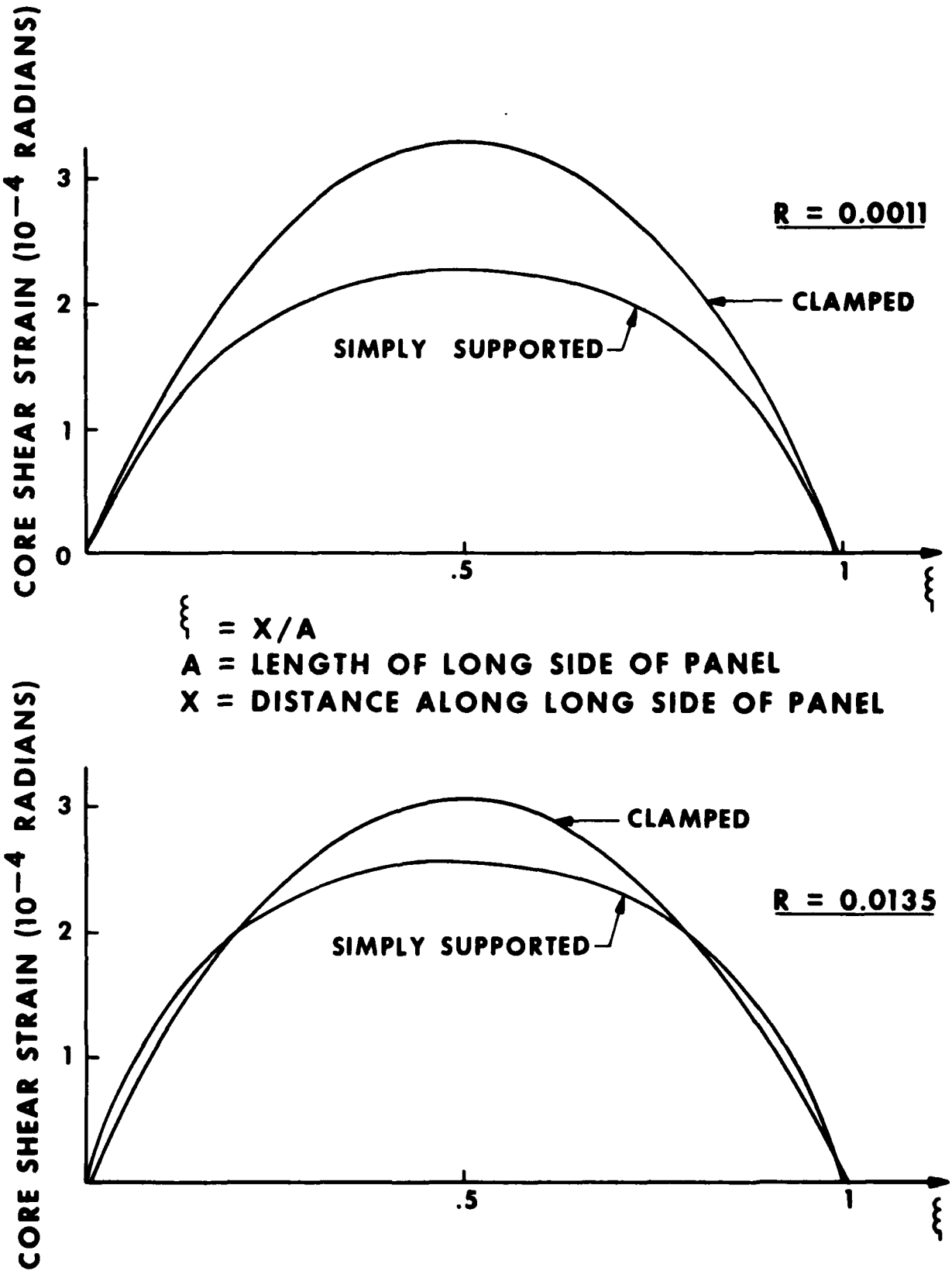

Figure 12 Transverse Core Shear Strain Along the Long Edge of Uniformly Loaded Rectangular Sandwich Panels with R = 0.0011 and R = 0.0135

The data recovery locations 6 and 7 shown in Figure 7 did not match up with any nodal locations in the finite element model. It was then necessary to process the finite element data to obtain predictions of displacement and strain at locations 6 and 7 in Figure 7. The displacements at locations 6 and 7 were computed using linear interpolation on the finite element nodal data. To compute the strains it was necessary to fit a quadratic polynomial to the finite element nodal rotations. These polynomials were used to compute the derivative of the nodal rotations ($\Phi_{x,x}$ or $\Phi_{y,y}$ in the appendix). Using the derivatives of the nodal rotations and the panel's extreme fiber distance ($C = 2.64 \cdot 10^{-2}$ m) the skin strains at the nodes were computed. The strains at locations 6 and 7 were then computed using linear interpolation on the nodal skin strain data. When a panel's displacements were measured (see reference 2) the displacement dial gages were attached to a rigid horizontal bar. The horizontal bar was rigidly attached to two vertical bars which stood on the top surface of the panel directly over the edge of the rectangular void. As the panel curled up in the corners the vertical supports moved. This type of error was accounted for in the computation of the total error in the displacements.

The results of these error calculations are given in Table 7. The errors in Table 7 are the theoretical errors expected in Tables 2 to 6 at locations 6 and 7 for the panel with $R = 0.0284$. Thus, one-half of the displacement errors at locations 6 and 7 in Table 2 can be accounted for by correcting boundary conditions and including the effects of mounting locations 6 are small and those for location 7 are large. A comparison of the finite element data for both boundary conditions indicates that the displacements are within 2.0% at locations 1 to 5 in Figure 7. Thus, these calculations indicate that the panel lifting off of the support will cause errors only at locations 6 and 7. Also, the theoretical assumption of the existence of a straight material line (see appendix) is a poor assumption near the boundary when the experimental data is to be matched. This theoretical assumption implies that the shear load is transferred to the boundary uniformly through the entire thickness of the panel. In the experiment the shear load is transferred to the boundary through only the bottom skin of the panel. This difference of load transfer methods could also be a cause of strain errors at locations 6 and 7 in Figure 7. The large errors at locations 6 and 7 in Tables 2 to 6 and the above discussion on errors resulting from approximating panel boundary conditions implies the following. When sandwich panels are analyzed in Army shelters the panel boundaries should be given special consideration when the analysis data is being used for design purposes.

4. CONCLUSIONS:

The conclusions given below relate to the accuracy of the sandwich panel bending theory described in the appendix when it is used to predict the bending behavior of the sandwich panels tested in references 2 and 6 studied in this report.

a. The center deflection of both square and rectangular aluminum skin-aluminum honeycomb core sandwich panels as described in section 2 can be computed with an error in the range of ±10.0%.

b. The failure load of both square and rectangular aluminum skin-aluminum honeycomb core sandwich panels designed to fail in core shear can be computed with an error in the range of +10.0% to −50.0%. The majority of the panels tested were stronger than the theory indicated.

TABLE 7

Errors from Panel Lifting Off Foundation

These results apply to Panels 1 and 2 of Reference 2.

For these panels R = 0.0284 = Shear Flexibility/Total Flexibility.

Pressure = 60 kPa.

See Figure 12 for location numbers.

D_A = Data for case when panel is allowed to lift off foundation.

D_B = Data for case when panel is simply supported.

$$\% \text{ Error} = 100 \left[\frac{D_B - D_A}{D_A} \right]$$

Top skin strain = Bottom skin strain for these calculations.

	% ERROR		
Location	Vertical Displacement*	Skin Strain Short Direction**	Skin Strain Long Direction***
6	–34.	– 5.3	4.5
7	–34.	–23.	–82.

*Compare with Table 2

**Compare with Tables 3 and 4

***Compare with Tables 5 and 6

c. The error in the failure load predictions of b, above, is related to the theoretical material line rotation at the center of the long edge of the rectangular panels. The larger the material line rotation, the larger the error (and the stronger the panel).

d. The maximum computed transverse shear strain at the center of the long edge of the rectangular panels of c, above, for clamped boundary conditions is larger than the same shear strain for simply supported boundary conditions. This result implies that an experimental clamping action was not the cause of the large errors in prediction of the failure load.

e. Finite element solutions using the NASTRAN (15.5) plate bending element with isotropic transverse shear properties for the core agree well with the analytical solutions which include the effects of both core shear moduli. The errors are in the range of ±10.0% for both the center deflection and the material line rotation at the center of the long edge.

f. The vertical displacements of the rectangular aluminum skin-paper honeycomb core panels (as described in section 2) can be computed with an error in the range of +5.% to −10.% everywhere on the panel except at the ends of the panel. The theory usually underestimates the deflection.

g. The skin strains for the aluminum skin-paper honeycomb core panels in the short span direction measured at the center of the panel can be computed with an error in the range of +5.% to −20.%. The theory usually underestimates the strain.

h. The skin strains for the aluminum skin-paper honeycomb core panels, computed from the simple bending theory, in the short span direction at the center of the long edge of the panel are not reliable since the errors were of large magnitude and did not have a consistent sign.

i. The computed skin strains for the aluminum skin-paper honeycomb core panels in the long span direction were incorrect at all locations on the panel. However, these strains were small and would not be important for design work. The errors were usually larger than 10.0%.

j. The theory predicts that if the aluminum skin-paper honeycomb core panels are allowed to lift off of the supporting foundation then large errors will result near the end of the panels. Displacement and strain errors will be large in the corners of the panel as a result of the changing boundary conditions and displacement errors will also be large all across the end of the panel as a result of mounting displacement measuring equipment on the panels corners.

k. The sandwich panel theory can be used to predict displacements, failure loads, and skin strains within the accuracy required for design of Army tactical shelters. The NASTRAN (15.5) CQDPLT element approximates the sandwich panel theory within the accuracy required for design when large aluminum skin-paper honeycomb core sandwich panels are analyzed.

REFERENCES

1. A. R. Johnson and V. P. Ciras. Finite Element Analysis of a Statically Loaded ISO Tactical Shelter. Technical Report NATICK/TR–79/023, US Army Natick Research & Development Command, Natick, MA, 1979.

2. F. Barca. Experimental Measurement of Strain and Deflection in a Uniformly Loaded Simply Supported Composite Panel. Technical Report NATICK/TR–79/018, US Army Natick Research & Development Command, Natick, MA, 1979.

3. F. Barca. Experimental Measurement of Strain and Acceleration Levels in a Rigid-Wall Shelter Subjected to Environmental Loadings. Technical Report NATICK/TR–79/024, US Army Natick Research & Development Command, Natick, MA, 1978.

4. Richard H. MacNeal. The NASTRAN Theoretical Manual (Level 15), COSMIC. University of Georgia, Georgia, April 1972. Chapter 15.

5. M. E. Raville. Deflection and Stresses in a Uniformly Loaded Simply Supported Rectangular Sandwich Plate. Department of Agriculture, Forest Products Laboratory, No. 1847, December 1955.

6. W. C. Lewis. Supplement to Deflection and Stresses in a Uniformly Loaded Simply Supported Rectangular Sandwich Plate, Experimental Verification of Theory. Department of Agriculture, Forest Products Laboratory, No. 1847A, December 1956.

7. T. W. Reichard. Mechanical Properties of Paper Honeycomb for Use in Military Shelters. NBS Report 10 544, National Bureau of Standards, Washington, D.C., February 1971.

8. Military Standardization Handbook MIL-HDBK-5C, Metallic Materials and Elements for Aerospace Vehicle Structures, 15 September 1976.

9. J. M. Whitney and N. J. Pagano. "Shear Deformation in Heterogeneous Anisotropic Plates," Journal of Applied Mechanics, Vol 37, Series E, No. 4, 1970, pp 1031–1036.

APPENDIX

Analysis of Rectangular Sandwich Panels for Thin-Skin/Thick-Core Assumptions

INTRODUCTION:

From the late 1940's to the present time an extensive amount of research work has been done on the analysis of composite plates. Although sophisticated analysis techniques are available, the effort required to apply them to practical design problems is often large. The purpose of this analysis is to mathematically describe the bending behavior of sandwich panels used in tactical shelters in the best formulation for comparing experimentally measured and theoretically computed data. Since the output stress data from finite element programs is only available at the geometric center of the elements, it is difficult to use the finite element data when comparing experimental and theoretical data. For this reason, and analytical solution was desired. The techniques developed by Whitney and Pagano[9] were used to obtain the Fourier solution described below. The assumptions of this thin-skin/thick-core model are closely related to the assumptions made for the plate element in level 15.5 of the NASTRAN computer program. Thus, the comparison of experimental and theoretical data made on the basis of the Fourier solution also applies to NASTRAN (15.5) finite element solutions.

FOURIER ANALYSIS:

The sandwich plate is assumed to be made of isotropic high moduli thin skins adhered to a low moduli thick core. The core is assumed to deform in transverse shear only and the skins are used to determine the bending neutral surface. Figure A1 shows the basic coordinate system to be used for this analysis. The material displacements, u, v, and w are measured parallel to the basic x, y, and z coordinate axes. The simplest approximation to the material displacement fields is given by the following relations (see Figures A2 and A3):

$$\begin{aligned} u(x, y, z) &= -z\ \Phi_x(x,y) \\ v(x, y, z) &= -z\ \Phi_y(x,y) \\ w(x, y, z) &= w(x,y) \end{aligned} \qquad \text{(A-1)}$$

In (A-1) Φ_x and Φ_y are generalized coordinates locating the material line after deformation, and w locates the bending neutral surface.

[9] J. M. Whitney and N. J. Pagano. "Shear Deformation in Heterogeneous Anisotropic Plates," Journal of Applied Mechanics, Vol 37, Series E, No. 4, 1970, pp 1031–1036.

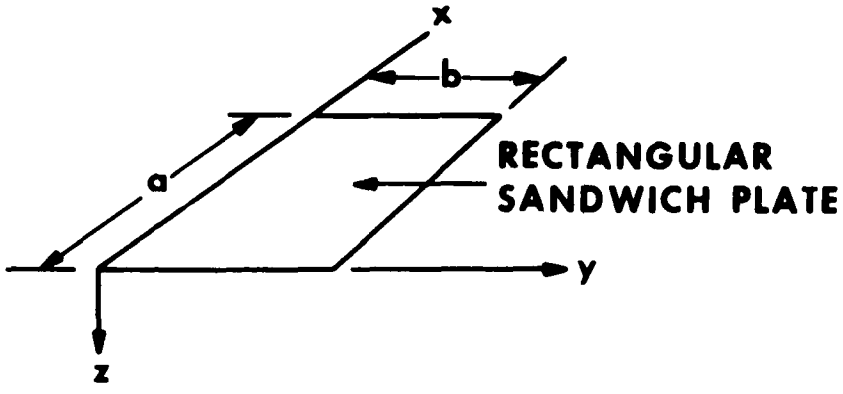

Figure A1 Basic Coordinate System

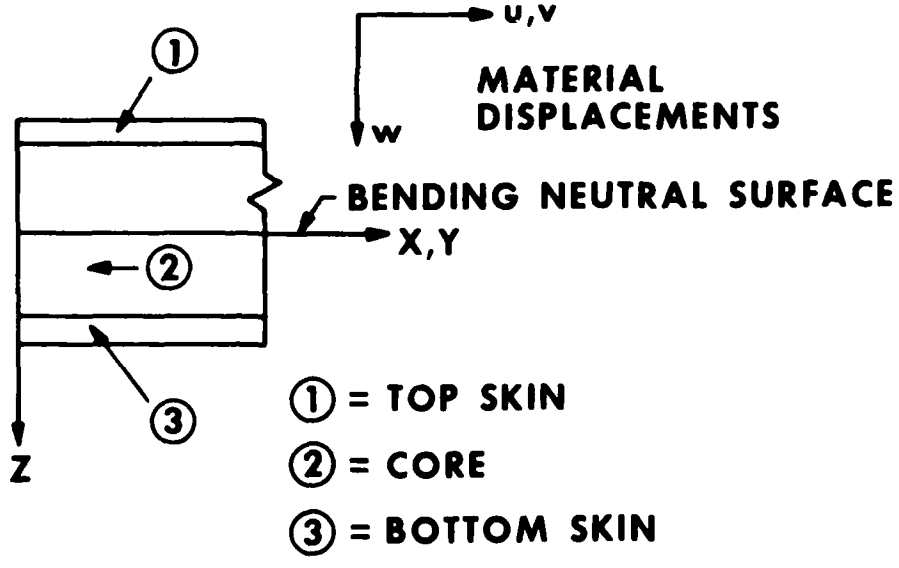

Figure A2 Location of Layers

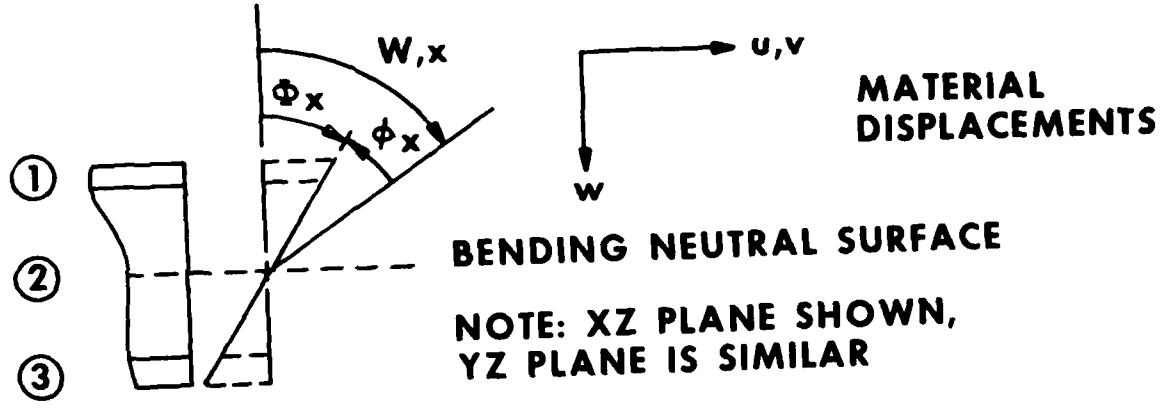

W,x = ROTATION ANGLE OF NORMAL TO NEUTRAL SURFACE
φx = SHEAR ANGLE
Φx = GENERALIZED COORDINATE LOCATING MATERIAL LINE

Figure A3 Generalized Coordinates

The linear strain displacement relations are used, and for this model are given for the skins as

$$\epsilon_x = u_{,x}$$
$$\epsilon_y = v_{,y} \qquad \text{(A–2a)}$$
$$\gamma_{xy} = u_{,y} + v_{,x}$$

and for the core

$$\gamma_{xz} = u_{,z} + w_{,x}$$
$$\gamma_{yz} = v_{,z} + w_{,y} \qquad \text{(A–2b)}$$

The stress-strain relations for the skin are

$$\sigma_x = D_{11}\epsilon_x + D_{12}\epsilon_y$$
$$\sigma_y = D_{12}\epsilon_x + D_{22}\epsilon_y \qquad \text{(A–3a)}$$
$$\tau_{xy} = G_{xy}\gamma_{xy}$$

and for the core

$$\tau_{xy} = G_{xy}\gamma_{xy}$$
$$\tau_{yz} = G_{yz}\gamma_{yz} \qquad \text{(A–3b)}$$

Assuming a loading function q(x,y) which acts in the Z direction, the potential energy of the panel can be expressed as shown in (A–4)

$$\Pi = \frac{1}{2} \int\int\int \left(\sigma_x\epsilon_x + \sigma_y\epsilon_y + \tau_{xy}\delta_{xy} \right) \, dxdydz$$
$$+ \frac{1}{2} \int\int\int \left(\tau_{xy}\gamma_{xy} + \tau_{yz}\gamma_{yz} \right) \, dxdydz \qquad \text{(A–4)}$$
$$- \int\int qwdxdy$$

Substituting (A–1), (A–2) and (A–3) into the first term in (A–4) and integrating over the thickness of the panel yields equation (A–5).

$$\Pi = \frac{1}{2} \int\int \Big(D_{11}\Phi^2{}_{x,x} + 2D_{12}\Phi_{x,x}\Phi_{y,y} + D_{22}\Phi^2{}_{y,y}$$
$$+ G_{12} \, (\Phi_{x,y} + \Phi_{y,x})^2 + G_{xz} \, (w_{,x} - \Phi_x)^2 \qquad \text{(A–5)}$$
$$+ G_{yz} \, (w_{,y} - \Phi_y)^2 - 2\,qw \Big) \, dxdy$$

In expression (A–5) $D_{11}, D_{12} \ldots, G_{yz}$ are the panel constants which result from integrating over the thickness of the panel. For the simply supported rectangular panel indicated in Figure A1, a simple application of the calculus of variations produces the following equilibrium equations and boundary conditions from equation (A–5);

Equilibrium Equations:

$$G_{xz}w_{,xx} + G_{yz}w_{,yy} - G_{xz}\Phi_{x,x} - G_{yz}\Phi_{y,y} = -q \qquad \text{(A–6)}$$

$$G_{xz}w_{,x} + D_{11}\Phi_{x,xx} + G_{12}\Phi_{x,yy} - G_{xz}\Phi_x + (D_{12} + G_{12})\Phi_{y,xy} = 0$$

$$G_{yz}w_{,y} + (D_{12} + G_{12})\Phi_{x,xy} + D_{22}\Phi_{y,yy} + G_{12}\Phi_{y,xx} - G_{yz}\Phi_y = 0$$

Boundary Conditions for a Side Parallel to the X-axis: (y = o,b)

$$G_{yz}(w_{,y} - \Phi_y)\delta w = 0$$

$$G_{12}(\Phi_{x,y} + \Phi_{y,x})\delta\Phi_x = 0 \qquad \text{(A–7)}$$

$$(D_{22}\Phi_{y,y} + D_{12}\Phi_{x,x})\delta\Phi_y = 0$$

Boundary Conditions for a Side Parallel to the Y-axis: (x = o,a)

$$G_{xy}(w_{,x} - \Phi_x)\delta w = 0$$

$$(D_{11}\Phi_{x,x} + D_{12}\Phi_{y,y})\delta\Phi_x = 0 \qquad \text{(A–8)}$$

$$G_{12}(\Phi_{x,y} + \Phi_{y,x})\delta\Phi_y = 0$$

If the rectangular panel is simply supported then the coefficients of the generalized coordinate variations $\delta\Phi_x$ and $\delta\Phi_y$ in (A–7) and (A–8) must vanish. The vanishing of these coefficients and the solution to the differential equations (A–6) is easily obtained if the load, q, can be expanded in a Fourier series (see reference 1). The solution is expressed as follows:

$$w = \sum_{m=1}^{\infty}\sum_{n=1}^{\infty} w_{mn} \operatorname{Sin}\frac{m\pi x}{a} \operatorname{Sin}\frac{n\pi y}{b}$$

$$\Phi_x = \sum_{m=1}^{\infty}\sum_{n=1}^{\infty} \Phi_{xmn} \operatorname{Cos}\frac{m\pi x}{a} \operatorname{Sin}\frac{n\pi y}{b} \qquad \text{(A–9)}$$

$$\Phi_y = \sum_{m=1}^{\infty}\sum_{n=1}^{\infty} \Phi_{ymn} \operatorname{Sin}\frac{m\pi x}{a} \operatorname{Cos}\frac{n\pi y}{b}$$

$$q = \sum_{m=1}^{\infty}\sum_{n=1}^{\infty} Q_{mn} \operatorname{Sin}\frac{m\pi x}{a} \operatorname{Sin}\frac{n\pi y}{b}$$

Substitution of (A–9) into (A–7) and (A–8) indicates that the boundary conditions are identically satisfied and substitution of (A–9) into (A–6) yields three infinite series whose sums must be identically zero. These series are constructed from orthogonal functions which are dependent upon m and n. Thus, the coefficients in these series must vanish. Collecting the coefficients with common m's and n's leads to the following condition on the coefficients:

$$\begin{bmatrix} -G_{xz}\left(\frac{m\pi}{a}\right)^2 - G_{yz}\left(\frac{n\pi}{b}\right)^2 & G_{xz}\left(\frac{m\pi}{a}\right) & G_{yz}\left(\frac{n\pi}{b}\right) \\ G_{xz}\left(\frac{m\pi}{a}\right) & -D_{11}\left(\frac{m\pi}{a}\right)^2 - G_{12}\left(\frac{n\pi}{b}\right)^2 - G_{xz} & -(D_{12}+G_{12})\left(\frac{m\pi}{a}\right)\left(\frac{n\pi}{b}\right) \\ G_{yz}\left(\frac{n\pi}{b}\right) & -(D_{12}+G_{12})\left(\frac{m\pi}{a}\right)\left(\frac{n\pi}{b}\right) & -D_{22}\left(\frac{n\pi}{b}\right)^2 - G_{12}\left(\frac{m\pi}{a}\right)^2 - G_{yz} \end{bmatrix} \begin{bmatrix} w_{mn} \\ \Phi_{xmn} \\ \Phi_{ymn} \end{bmatrix} = \begin{bmatrix} Q_{mn} \\ 0 \\ 0 \end{bmatrix} \tag{A–10}$$

To simplify the notation (A–10) can be written as follows:

$$\begin{bmatrix} A_1 & A_2 & A_3 \\ A_2 & A_4 & A_5 \\ A_3 & A_5 & A_6 \end{bmatrix} \begin{bmatrix} w_{mn} \\ \Phi_{xmn} \\ \Phi_{ymn} \end{bmatrix} = \begin{bmatrix} Q_{mn} \\ 0 \\ 0 \end{bmatrix} \tag{A–11}$$

The solution of (A–11) is given by the following relations:

$$w_{mn} = \frac{Q_{mn}}{A_1 - \dfrac{A_2^2 A_6 + A_3^2 A_4 - 2A_2 A_3 A_5}{A_4 A_6 - A_5^2}}$$

$$\Phi_{xmn} = -\left[\frac{A_2 A_6 - A_3 A_5}{A_4 A_6 - A_5^2}\right] w_{mn} \tag{A–12}$$

$$\Phi_{ymn} = -\left[\frac{A_3 A_4 - A_2 A_5}{A_4 A_6 - A_5^2}\right] w_{mn}$$

If the Fourier expansion of the load q(x,y) is known then (A–12) gives the coefficients for the Fourier expansion of the generalized coordinates when the plate is in static equilibrium. Substitution of the Fourier expansions into (A–1) through (A–3) yields the stress state in the sandwich panel.

RELATION TO NASTRAN CQDPLT ELEMENT:

The analysis of complete tactical shelters requires the use of finite element methods. Since this study emphasizes the comparison of measured data to analytical solutions, it is also necessary to determine the numerical relation between the analytical and approximate finite element solutions. In order to make this comparison it is necessary to investigate the theoretical connection between the analytical and finite element models and then to investigate the relation between actual solutions obtained by each method.

The transverse shear strains for the thin-skin/thick-core analytical model (model No. 1) are expressed in terms of the generalized coordinates by using Figure A3, and equations (A–1) and (A–2). The results are given in (A–13).

$$\gamma_{xz} = w_{,x} - \Phi_x$$

$$\gamma_{yz} = w_{,y} - \Phi_y \qquad \text{(A–13)}$$

Comparing (A–14) with the definition of the generalized coordinates used in the derivation of the NASTRAN CQDPLT finite element stiffness matrix (see reference 4) we see that the displacement relations are the same in each case. Substituting the generalized coordinates into the expressions used in the definition of the strain energy in the NASTRAN plate element leads to equation (A–14). This equation is identical to the strain energy portion of equation (A–5) except that the core must have isotropic transverse shear properties in NASTRAN. Thus, if the same plate constants are used in the Fourier model and finite element models, the same answers should be obtained (convergence of the finite element method considered).

$$V = \frac{1}{2} \int \Big(D_{11}\Phi_{x,x}^2 + 2D_{12}\Phi_{x,x}\Phi_{y,y} + D_{22}\Phi_{y,y}^2 + G_{12}(\Phi_{x,y} + \Phi_{y,x})^2 + Gt\gamma_{xy}^2 + Gt\gamma_{yz}^2 \Big)\, dA \qquad \text{(A–14)}$$